Gas Sorption, Diffusion, and Permeation in Poly(2,2-bis(trifluoromethyl)-4,5-difluoro-1,3-dioxole-*co*-tetrafluoroethylene)

T. C. Merkel,† V. Bondar,† K. Nagai,† B. D. Freeman,*,† and Yu. P. Yampolskii‡

Department of Chemical Engineering, North Carolina State University, Campus Box 7905, Raleigh, North Carolina 27695-7905, and Institute of Petrochemical Synthesis, Russian Academy of Sciences, 29 Leninsky Pr., 117912, Moscow, Russia

Received May 3, 1999; Revised Manuscript Received September 13, 1999

ABSTRACT: The solubility and permeability of H_2, O_2, N_2, CO_2, CH_4, C_2H_6, C_3H_8, CF_4, C_2F_6, and C_3F_8 in TFE/BDD87, a random copolymer prepared from 87 mol % 2,2-bis(trifluoromethyl)-4,5-difluoro-1,3-dioxole [BDD] and 13 mol % tetrafluoroethylene [TFE], are reported as a function of temperature and pressure. Sorption isotherms of all penetrants except hydrogen are concave to the pressure axis and are well-described by the dual-mode model. Hydrogen exhibits linear sorption isotherms. In contrast to previous results in hydrocarbon-rich polymers, the solubility of perfluorocarbon penetrants is higher in TFE/BDD87 than that of their hydrocarbon analogues. The solubility of all penetrants in TFE/BDD87 decreases with increasing temperature. Enthalpies of sorption become more negative as penetrant size increases. Fluorocarbon enthalpies of sorption at infinite dilution are significantly more exothermic than those of their hydrocarbon analogues, suggesting more favorable interactions between fluorocarbon penetrants and perfluorinated TFE/BDD87 than between hydrocarbon penetrants and this polymer. Perfluorocarbon permeability coefficients are nearly an order of magnitude lower than those of their hydrocarbon analogues due to the larger size of the fluorocarbons and their subsequently lower diffusivities. The permeability of TFE/BDD87 increases with increasing temperature, indicating that activation energies of permeation (E_p) are positive. E_p values in TFE/BDD87 are smaller than those of conventional glassy polymers. Diffusion coefficients of the lower sorbing gases (O_2, N_2, CO_2, CH_4, CF_4) exhibit a concentration dependence that is consistent with dual-mode transport in unplasticized glassy polymers. For more strongly sorbing C_2H_6, C_3H_8, C_2F_6, and C_3F_8, diffusion coefficients increase exponentially with increasing penetrant concentration, suggesting plasticization. Activation energies of diffusion in TFE/BDD87 are positive and increase linearly with penetrant diameter squared. Relative to conventional glassy polymers, E_D values in TFE/BDD87 are low. However, $|E_D|$ is larger than $|\Delta H_S|$. TFE/BDD87 is easily plasticized by the larger, more soluble penetrants and is susceptible to penetrant-induced conditioning. The level of conditioning is highest for the largest, most soluble penetrant examined (C_3F_8), and the conditioned state gradually relaxes toward that of the as-cast state.

Introduction

In membrane-based gas and vapor separation applications, polymeric materials that exhibit high permeability, high selectivity, and long-term transport property stability under process conditions are desired.[1] Additionally, a membrane must also be stable in process environments. For example, in the manufacture of perfluorocarbons [PFCs] via electrochemical fluorination of hydrocarbons in hydrofluoric acid [HF], a waste gas composed of hydrogen with smaller amounts of perfluorocarbons and HF is produced.[2] Economic and environmental considerations favor recovery of the perfluorocarbons. However, few polymers are stable in a chemically challenging environment such as that presented by HF.

Poly(tetrafluoroethylene) [PTFE] is among the most chemically resistant polymers known. However, this semicrystalline polymer exhibits very low permeability to gases. For example, the permeability coefficient of nitrogen in PTFE at 25 °C is 1.3 barrers, where 1 barrer $= 10^{-10}$ cm^3 (STP) cm/(cm^2 s cmHg).[3] In comparison, nitrogen permeability coefficients in poly(dimethylsiloxane) [PDMS], a highly permeable rubbery polymer, and poly(1-trimethylsilyl-1-propyne) [PTMSP], a stiff chain glassy polymer, are 390 and 6800 barrers, respectively.[4,5]

Random copolymerization of tetrafluoroethylene [TFE] with sufficient amounts of 2,2-bis(trifluoromethyl)-4,5-difluoro-1,3-dioxole [BDD] produces amorphous, high glass transition copolymers that are among the most permeable polymers known[6] and have the excellent chemical resistance associated with fluoropolymers.[7] The TFE and BDD repeat units are

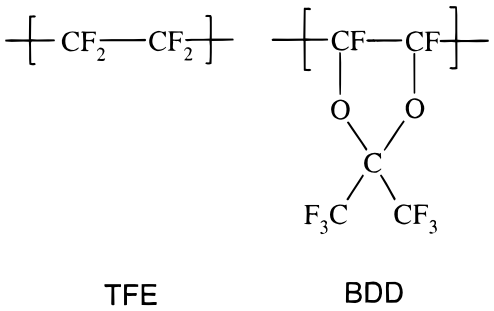

TFE BDD

The high permeability coefficients in these copolymers are attributed, in part, to extremely high fractional free volumes (FFVs). For example, the FFV of the fluorocopolymer composed of 13 mol % tetrafluoroethylene and 87 mol % 2,2-bis(trifluoromethyl)-4,5-difluoro-1,3-dioxole (TFE/BDD87, trade name AF2400) is 0.32 based on a density of 1.74 g/cm^3.[7] This value is among the

† North Carolina State University.
‡ Russian Academy of Sciences.
* Corresponding author.

10.1021/ma990685r CCC: $18.00
Published on Web 11/24/1999

highest ever reported for a dense polymer and is similar to that of PTMSP, the most permeable polymer known.[8] In comparison, the FFV of polysulfone, a conventional glassy polymer used in permanent gas separations, is only 0.16.[9]

The light gas, hydrocarbon, and chlorofluorocarbon permeation properties of TFE/BDD87 have been reported.[6,10] However, a systematic series of gas sorption data or the temperature dependence of transport properties in TFE/BDD87 are not available. This study reports the temperature dependence of transport properties, including solubility, in TFE/BDD87 for a series of light gases, hydrocarbons, and perfluorocarbons.

The choice of perfluorocarbon penetrants was stimulated by growing industrial interest in the separation and recovery of these compounds from waste streams. Recent studies focusing on recovering perfluorinated compounds from the exhaust of semiconductor wafer cleaning processes have demonstrated that CF_4, C_2F_6, and C_3F_8 can be separated from permanent gases, such as nitrogen, using polymer membrane separation technology.[11] However, there are very few fundamental data regarding PFC transport properties in polymers.

Recently, the sorption, diffusion, and permeation properties of a series of perfluorocarbons in two hydrocarbon-rich polymers, rubbery PDMS and high free volume, glassy PTMSP, were reported.[4,5] In these polymers, PFC permeability coefficients are more than an order of magnitude lower than those of their hydrocarbon analogues and lower even than those of the permanent gases. In PDMS, this result was ascribed primarily to an unfavorable interaction between the hydrocarbon-rich PDMS matrix and PFC penetrants, which resulted in very low perfluorocarbon solubility in PDMS. In PTMSP, perfluorocarbon solubilities were also generally lower than those of their hydrocarbon analogues, but the difference was not as great as in PDMS. It was primarily the larger size of the perfluorocarbons, relative to their hydrocarbon analogues, that caused low PFC diffusivities and permeabilities in PTMSP.

This paper extends the previous work with PDMS and PTMSP to include investigation of PFC transport properties in a perfluorinated polymer. The sorption and permeability of TFE/BDD87 to a series of gases and vapors, including CF_4, C_2F_6, C_3F_8, and their hydrocarbon analogues, are reported as a function of temperature in TFE/BDD87. These data are used to calculate the temperature dependence of penetrant diffusion coefficients. The composite results are interpreted using current theories of penetrant solubility, diffusivity, permeability, and the temperature dependence of these properties in glassy polymers.

Background

The permeability, P, of a polymer to a penetrant is[1]

$$P = \frac{Nl}{p_2 - p_1} \tag{1}$$

where p_2 is feed (or upstream) pressure, p_1 is permeate (or downstream) pressure, l is film thickness, and N is the steady-state penetrant flux through the polymer film.

For a nonporous polymer membrane, gas transport is commonly described by a three-step solution-diffusion mechanism. When penetrant flux obeys Fick's law, the permeability coefficient, P, can be expressed as[1]

$$P = \left(\frac{C_2 - C_1}{p_2 - p_1}\right)\bar{D} \tag{2}$$

where $\bar{D}$ is the concentration-averaged diffusivity and C_2 and C_1 are the penetrant concentrations in the polymer at the upstream and downstream faces of the membrane, respectively. When the downstream pressure (p_2) is much less than the upstream pressure (p_1), the term in parentheses in eq 2 becomes C_2/p_2, which is the solubility coefficient, S, at the upstream pressure. The concentration-averaged diffusivity is defined by[1]

$$\bar{D} = \int_{C_1}^{C_2} \frac{D}{1 - w}\,\mathrm{d}C = \int_{C_1}^{C_2} D_{\mathrm{eff}}\,\mathrm{d}C \tag{3}$$

where D is the local concentration-dependent diffusion coefficient, w is the mass fraction of penetrant in the polymer at concentration C, and D_{eff} is the so-called local effective diffusion coefficient.

Penetrant sorption in glassy polymers is frequently described by the dual-mode model:[12]

$$C = k_{\mathrm{D}}p + \frac{C'_{\mathrm{H}}bp}{1 + bp} \tag{4}$$

where C is the equilibrium penetrant concentration in the polymer at pressure p, k_{D} is the Henry's law parameter describing penetrant dissolution into the equilibrium densified polymer matrix, and C'_{H} is the Langmuir capacity parameter, which describes the sorption capacity of the nonequilibrium excess free volume characteristic of the glassy state. The Langmuir affinity parameter, b, is an equilibrium constant describing the affinity of a penetrant for a Langmuir site. In terms of the dual-mode model, the solubility coefficient, S, may be expressed as

$$S = \frac{C}{p} = k_{\mathrm{D}} + \frac{C'_{\mathrm{H}}b}{1 + bp} \tag{5}$$

The temperature dependence of permeability, diffusivity, and solubility at temperatures removed from polymer thermal transitions is described as follows:[1]

$$P = P_0 \exp\left[-\frac{E_{\mathrm{p}}}{RT}\right] \tag{6}$$

$$D = D_0 \exp\left[-\frac{E_{\mathrm{D}}}{RT}\right] \tag{7}$$

$$S = S_0 \exp\left[-\frac{\Delta H_{\mathrm{S}}}{RT}\right] \tag{8}$$

where P_0, D_0, and S_0 are preexponential constants, E_{p} is the activation energy of permeation, E_{D} is the activation energy of diffusion, and ΔH_{S} is the enthalpy of sorption. As permeability is the product of solubility and diffusivity, the following relationship exists between the activation energies of permeation and diffusion and the enthalpy of sorption:

$$E_{\mathrm{p}} = E_{\mathrm{D}} + \Delta H_{\mathrm{S}} \tag{9}$$

Experimental Section

Materials. TFE/BDD87, trade name AF2400, was purchased from DuPont (Newark, DE) and used as received. It is a random copolymer synthesized from 87 mol % 2,2-bis-

(trifluoromethyl)-4,5-difluoro-1,3-dioxole [BDD] and 13 mol % tetrafluoroethylene [TFE]. 50 μm thick isotropic films of TFE/BDD87 were cast from 1 wt % polymer solution in PF 5060, a perfluorinated solvent supplied by 3M (Minneapolis, MN). The films were dried at ambient conditions until a constant weight was achieved (at least 24 h). These films were utilized for the pure gas permeation and sorption experiments.

The gases and vapors had a purity of at least 99.5%. CO_2, O_2, and H_2 were purchased from Linde (Somerset, NJ). N_2, CH_4, C_2H_6, and C_3H_8 were obtained from National Specialty Gases (Raleigh, NC). CF_4 and C_2F_6 were supplied by Scott Specialty Gases (Durham, NC), and C_3F_8 was kindly provided by the 3M Company (Minneapolis, MN). All gases were used as received.

Permeation Measurements. The permeation properties of TFE/BDD87 were determined utilizing a constant pressure/variable volume apparatus.[13] The surface area of the film was 13.8 cm^2. For all penetrants except C_3H_8 and C_3F_8, upstream pressure was varied between 15 and 240 psig, and the downstream pressure was atmospheric (0 psig). For C_3H_8 and C_3F_8, the maximum upstream pressures were 50 and 120 psig, respectively. Gas flow rates were measured with a soap-film bubble flowmeter. The experimental temperature was maintained within ±0.5 °C with a DYNA-SENSE temperature control system. Prior to each experiment, both the upstream and downstream sides of the permeation cell were purged with penetrant gas. The permeability coefficients of gases and vapors were determined in the following order: H_2, O_2, N_2, CO_2, CH_4, C_2H_6, C_3H_8, CF_4, C_2F_6, C_3F_8. To avoid any conditioning effects due to the previous permeation test, fresh TFE/BDD87 films were used after testing each of the larger, more condensable vapors (CO_2, C_2H_6, C_3H_8, C_2F_6, C_3F_8). When steady-state conditions were achieved, the following expression was used to evaluate permeability:

$$P = \frac{l}{p_2 - p_1}\frac{273}{TA}\frac{p_{atm}}{76}\left(\frac{dV}{dt}\right) \tag{10}$$

where p_2 is the upstream pressure, p_1 is the downstream pressure (atmospheric pressure in this case), p_{atm} is atmospheric pressure (cmHg), A is the membrane area, T is the absolute temperature, and dV/dt is the volumetric displacement rate of the soap film in the bubble flowmeter.

Sorption Measurements. The solubility of gases and vapors in TFE/BDD87 was measured with a high-pressure barometric sorption apparatus.[14] Initially, a TFE/BDD87 film was placed in the sample chamber and exposed to vacuum overnight to remove air gases. Penetrant gas was then introduced into the chamber and allowed to equilibrate. Once the chamber pressure was constant, additional penetrant was introduced and equilibrium was reestablished. In this incremental manner, penetrant uptake was measured as a function of penetrant pressure. The maximum penetrant pressure was 4−27 atm depending on the penetrant. The order of penetrant measurement in the sorption experiments was the same as in the permeation experiments. Sorption equilibrium for all gases was reached within, at most, a few hours. The TFE/BDD87 film used in this work had previously been utilized to measure gas sorption isotherms.[15] N_2 isotherms determined before and after the sorption studies of the other penetrants agreed within experimental uncertainty, indicating no detectable long-term disruption of chain packing in this glassy polymer. After measuring each isotherm, the polymer sample was degassed overnight. The experimental temperature was maintained to within ±0.1 °C with a constant-temperature water bath.

Results and Discussion

Solubility. Sorption isotherms for H_2, O_2, N_2, CO_2, CH_4, C_2H_6, C_3H_8, CF_4, C_2F_6, and C_3F_8 in TFE/BDD87 are presented as a function of temperature in Figure 1a−j. Isotherms for all penetrants except hydrogen are concave to the pressure axis and are well-described by the dual-mode model at each temperature. Hydrogen exhibits linear sorption isotherms. The dual-mode sorption parameters for each penetrant (other than H_2) obtained by a nonlinear least-squares fit of eq 4 to the experimental data at 35 °C are recorded in Table 1. The slope of the hydrogen isotherm is reported in Table 1 as an effective Henry's law coefficient.

Table 1. Dual-Mode Sorption Parameters in TFE/BDD87 at 35 °C[a]

penetrant	k_D [cm^3 (STP)/(cm^3 atm)]	C'_H [cm^3 (STP)/cm^3]	b [1/atm]
H_2[b]	0.21		
O_2	0.21	44	0.015
N_2	0.11	38	0.015
CO_2	1.6	26	0.070
CH_4	0.35	25	0.036
C_2H_6	1.5	16	0.22
C_3H_8	4.2	13	0.83
CF_4	0.45	29	0.082
C_2F_6	1.6	18	0.59
C_3F_8	6.4	19	2.2

[a] The dual-mode parameters for H_2 and C_3F_8 are reported at 25 °C since the solubility of these penetrants was not measured at 35 °C. [b] k_D for H_2 is an effective Henry's law coefficient.

Sorption levels of all the penetrants examined are very high in TFE/BDD87, consistent with its extraordinary amount of free volume. As a comparison, Figure 2 presents N_2 sorption isotherms at 35 °C in TFE/BDD87, polycarbonate [PC], a conventional low free volume glassy polymer, poly(dimethylsiloxane) [PDMS], a highly permeable rubbery polymer, and poly(1-trimethylsilyl-1-propyne) [PTMSP], a high free volume glassy hydrocarbon-rich polymer. This comparison illustrates the exceptionally high gas solubility exhibited by TFE/BDD87 relative to conventional polymers. In fact, the sorption level of N_2 in TFE/BDD87 is similar to that in PTMSP, which has the highest light gas solubility of all polymers.[16]

In contrast to previous studies of hydrocarbon-rich polymers,[4,5] at a fixed pressure, the concentration of perfluorocarbon penetrant sorbed in TFE/BDD87 is higher than that of the analogous hydrocarbon penetrant. For example, at 15 atm and 35 °C the concentration of C_2F_6 sorbed in TFE/BDD87 (40 cm^3 (STP)/cm^3 polymer) is 13% higher than that of C_2H_6. In comparison, at the same temperature and pressure the concentration of C_2F_6 sorbed in hydrocarbon-rich PTMSP (45 cm^3 (STP)/cm^3 polymer) is half that of C_2H_6.[5] The difference in hydrocarbon and fluorocarbon solubilities is even greater in rubbery, hydrocarbon-rich PDMS, where under the same conditions the sorbed concentration of C_2F_6 (5.1 cm^3 (STP)/cm^3 polymer) is an order of magnitude lower than that of C_2H_6.[4] This solubility difference in liquidlike PDMS is similar to that in cyclohexane, a low molecular mass hydrocarbon liquid.[17] Thus, the difference between hydrocarbon and fluorocarbon solubilities in these media decreases in the order

$$\text{cyclohexane} \approx \text{PDMS} > \text{PTMSP} > \text{TFE/BDD87}$$

where in each case the polymer or liquid favors sorption of the chemically similar penetrant.

In the three hydrocarbon matrices (cyclohexane, PDMS, and PTMSP), penetrant−matrix interactions favor sorption of hydrocarbon penetrants over fluorocarbons. This result is consistent with the observations of Hildebrand and Scott,[17] who reported that hydrocarbon−fluorocarbon liquid mixtures exhibit anomalously

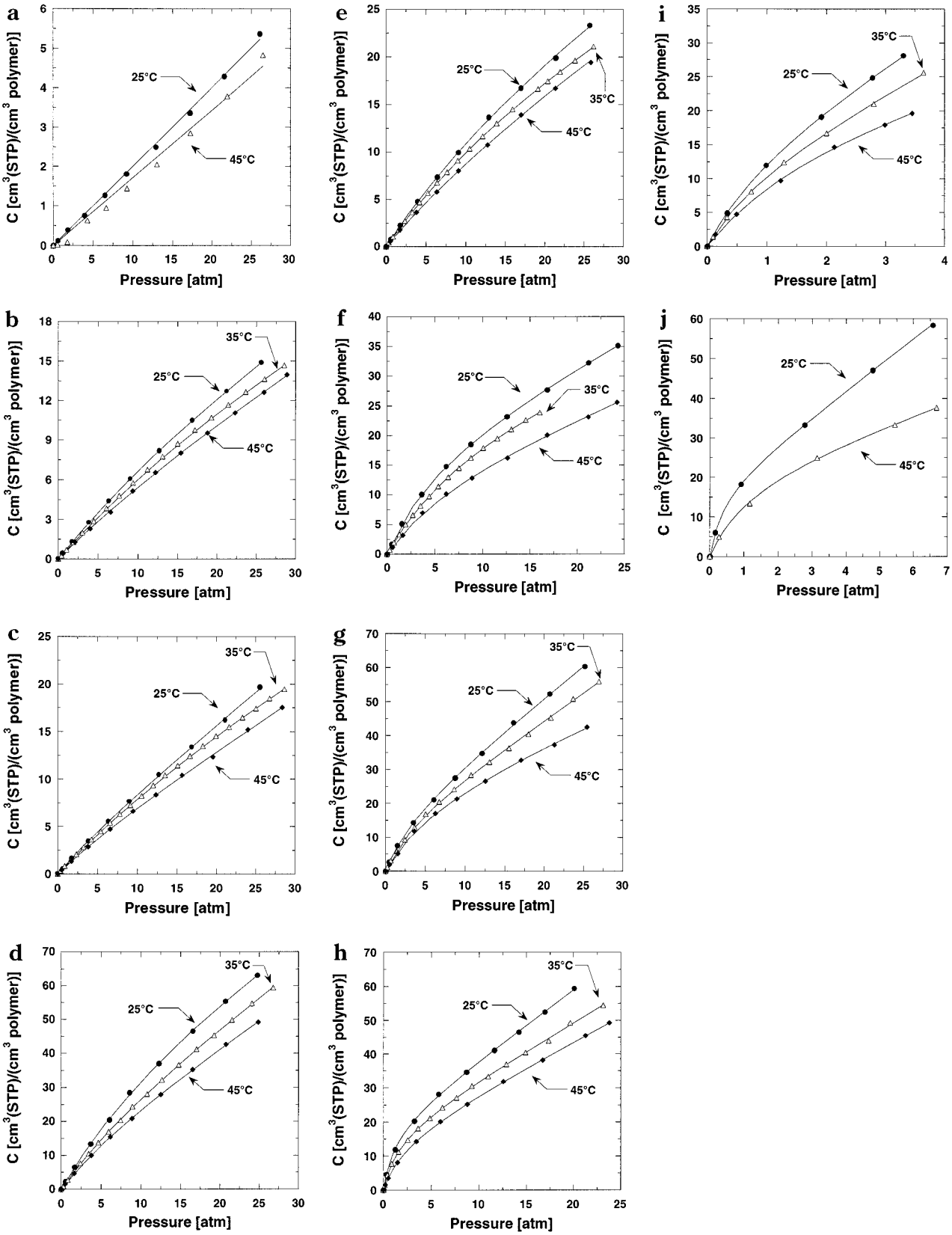

Figure 1. Sorption isotherms in TFE/BDD87: (a) H_2, (b) N_2, (c) O_2, (d) CO_2, (e) CH_4, (f) CF_4, (g) C_2H_6, (h) C_2F_6, (i) C_3H_8, (j) C_3F_8. The lines in (b)−(j) represent a least-squares fit of eq 4 to the experimental data.

large excess enthalpies of mixing. Hydrocarbon−fluorocarbon solubility differences are approximately the same in cyclohexane and PDMS, suggesting comparable penetrant−matrix interactions, which is consistent with the molecular level similarity of gas dissolution in a liquid and in a rubbery polymer. PTMSP, on the other hand, is a nonequilibrium glassy material with an enormous amount of excess free volume.[18] This nonequilibrium excess free volume is present as preexisting microvoids in the polymer matrix which are available for penetrant sorption. Since sorption into these sites requires little work to separate polymer chains to

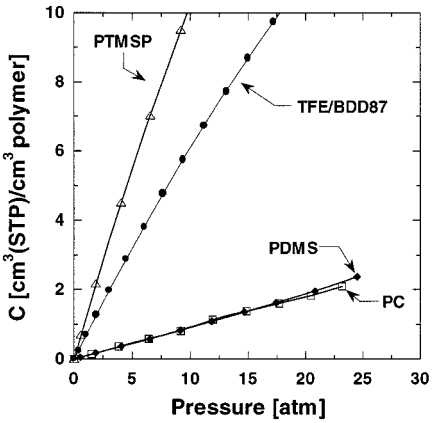

Figure 2. Comparison of nitrogen sorption isotherms in TFE/BDD87 [●], poly(1-trimethylsilyl-1-propyne) [PTMSP] [△], polycarbonate [PC] [□], and poly(dimethylsiloxane) [PDMS] [◆].

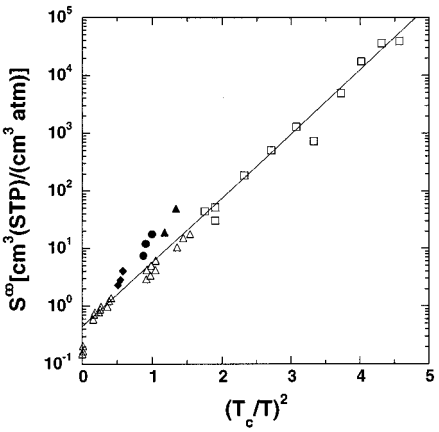

Figure 3. Penetrant infinite dilution solubility in TFE/BDD87 as a function of $(T_C/T)^2$: [△] hydrocarbon and permanent gas data of this study; [◆] CF_4 data of this study; [●] C_2F_6 data of this study; [▲] C_3F_8 data of this study; [□] hydrocarbon data of Bondar et al.[23]

accommodate penetrants, the effect of penetrant−polymer interactions on solubility is less important in PTMSP than in more densified media, such as a rubbery polymer or liquid. A previous study of hydrocarbon and fluorocarbon solubility in PTMSP supports this notion and suggests it is primarily the larger size of the fluorocarbons which inhibits their dissolution into PTMSP.[5] TFE/BDD87, like PTMSP, is a glassy polymer with a large amount of excess free volume. The slightly higher fluorocarbon solubilities in TFE/BDD87 relative to their hydrocarbon analogues suggest that in this polymer the effects of penetrant−polymer interactions, which favor fluorocarbon sorption, are more important than penetrant size effects, which favor sorption of the smaller hydrocarbon analogues.

From the sorption data, infinite dilution solubility coefficients, S^∞, were estimated for each penetrant by calculating the ratio of penetrant concentration to pressure in the limit as pressure approaches zero:

$$S^\infty = \lim_{p\to 0}\left(\frac{C}{p}\right) = k_D + C'_H b \qquad (11)$$

For H_2, the effective Henry's law coefficient recorded in Table 1 was used for S^∞. Solubility increases in the following order:

$$H_2 < N_2 < O_2 < CH_4 < CF_4 < CO_2 < C_2H_6 < C_2F_6 < C_3H_8 < C_3F_8$$

This is generally the order of increasing condensability of these penetrants. Several models of gas solubility in polymers have been developed that relate solubility to a measure of penetrant condensability. Gee[19] used classical thermodynamics to predict a linear relationship between the logarithm of gas solubility in amorphous polymers and penetrant critical temperature in the absence of specific polymer−penetrant interactions. Michaels and Bixler[20] proposed a similar relation using another measure of penetrant condensability, Lennard-Jones temperature, (ϵ/k), instead of critical temperature. Since we have measured penetrant solubility in TFE/BDD87 at several temperatures, it is desirable to determine whether a single correlation that incorporates the temperature dependence of solubility can describe all of the data. In this regard, Stern et al.[21,22] utilized a corresponding states approach to propose that the logarithm of S^∞ is a linear function of $(T_C/T)^2$ for a wide range of penetrants in polyethylene and poly(dimethylsiloxane).

Table 2. Comparison of Corresponding States Correlation Parameters

polymer	N	M^a	linear correl coeff, R
polyethylene	1.14	−1.36[b]	
poly(dimethylsiloxane)	1.075	−0.69[c]	
TFE/BDD87	1.11 ± 0.03	−0.35 ± 0.06	0.986

[a] With solubility in units of cm^3 (STP)/(cm^3 atm). [b] Calculated using an amorphous polyethylene density of 0.85 g/cm^3.[20] [c] Calculated using a poly(dimethylsiloxane) density of 1.138 g/cm^3.[22]

Figure 3 displays penetrant infinite dilution solubility in TFE/BDD87 as a function of $(T_C/T)^2$. Included in this figure are the solubilities of a series of higher hydrocarbons in TFE/BDD87 reported by Bondar et al.[23] The data in this figure can be represented by an equation of the form

$$\log(S^\infty) = M + N\left(\frac{T_C}{T}\right)^2 \qquad (12)$$

where N and M are adjustable parameters. The trend line in Figure 3 represents a least-squares fit of eq 12 to all of the solubility data. Table 2 compares the values of the parameters M and N obtained in this study with those reported by Stern et al. for polyethylene and poly(dimethylsiloxane). The slope of eq 12 is very similar for each of these polymers, while the intercept M exhibits more variation from polymer to polymer. This result is consistent with the variation in the parameters of the isothermal gas solubility correlations mentioned previously. The quantum gases (He and H_2) exhibit much lower solubility coefficients in TFE/BDD87 then expected on the basis of the correlation line in Figure 3. This result is consistent with a similar large deviation of helium solubility in polyethylene.[21] In TFE/BDD87, the three fluorocarbons have solubility coefficients that lie systematically above the correlation line. This result suggests a favorable interaction or affinity between the fluorocarbons and the perfluorinated TFE/BDD87 matrix relative to the interactions between the polymer matrix and the permanent gases and hydrocarbon vapors.

From Figure 1a−j, penetrant concentration decreases with increasing temperature, indicating the enthalpy

Table 3. Enthalpies of Sorption, Activation Energies of Permeation, and Activation Energies of Diffusion in TFE/BDD87 at Infinite Dilution

penetrant	H_2	O_2	N_2	CO_2	CH_4	C_2H_6	C_3H_8	CF_4	C_2F_6	C_3F_8
ΔH_S^∞ [kJ/mol]	−8.6	−8.7	−11.3	−14.8	−13.2	−14.2	−20.9	−22.0	−34.1	−37.5
E_p [kJ/mol]	3.1	6.3	8.9	0.9	9.8	21.2		22.7	31.1	
E_D[a] [kJ/mol]	11.7	15.0	20.2	15.7	23.0	35.4		44.7	65.2	

[a] E_D calculated as $E_p - \Delta H_S^\infty$.

of sorption is negative (i.e., exothermic) for all penetrants. The infinite dilution enthalpy of sorption, ΔH_S^∞, for each penetrant may be calculated from a van't Hoff plot of $\log(S^\infty)$ vs $1/T$. The results of these calculations are recorded in Table 3. The exothermic nature of penetrant sorption in TFE/BDD87 is consistent with previous reports of gas sorption in glassy polymers.[24,25] Penetrant dissolution into a polymer matrix can be envisioned as a two-step thermodynamic process: (1) penetrant condensation from a gas-phase density to a liquidlike density and (2) mixing of condensed penetrant (or, for supercritical gases, hypothetical condensed penetrant) with polymer segments.[1] Consequently, the enthalpy of sorption can be written as the algebraic sum of contributions from these two steps:[1]

$$\Delta H_S = \Delta H_{cond} + \Delta H_{mix} \qquad (13)$$

where ΔH_{cond} and ΔH_{mix} are the enthalpy changes associated with penetrant condensation and mixing, respectively. The enthalpy change associated with condensation is always negative (i.e., exothermic) and increases in magnitude as penetrant condensability (as measured by properties such as T_C) increases. In rubbery polymers, penetrant sorption requires creation of a molecular-scale gap in the polymer matrix, which is usually an endothermic process (i.e., $\Delta H_{mix} > 0$). For supercritical, permanent gases (i.e., H_2, He, etc.) the magnitude of ΔH_{cond} is usually much less than that of ΔH_{mix}, and subsequently, light gas solubility increases with increasing temperature.[1] Glassy polymers, such as TFE/BDD87, have nonequilibrium excess volume, generally described as so-called Langmuir microvoids.[24] At low penetrant pressures, most penetrant molecules sorb into these preexisting microvoids, which requires little or no energy ($\Delta H_{mix} \approx 0$) to generate gaps in the polymer matrix of sufficient size and shape to accommodate the penetrants. Consequently, ΔH_S may be negative (consistent with $\Delta H_{cond} < 0$), and light gas solubility decreases with increasing temperature.[25,26] For larger, more condensable gases and vapors, including many organic vapors, the sign and magnitude of ΔH_S are strongly influenced by the large contribution of ΔH_{cond}. As a result, vapor solubility in both rubbery and glassy polymers decreases with increasing temperature, and the temperature dependence of solubility often becomes stronger as T_C increases.

Figure 4a presents ΔH_S^∞ as a function of penetrant critical temperature in TFE/BDD87. On the basis of these data, enthalpies of sorption generally decrease (i.e., penetrant sorption becomes more exothermic) in TFE/BDD87 as T_C increases. This result is consistent with previous correlations of ΔH_S with penetrant condensability in both rubbery[27] and glassy[28] polymers. The fluorocarbon penetrants exhibit more exothermic enthalpies of sorption in TFE/BDD87 than anticipated on the basis of their condensability (as measured by T_C) and in fact fall on a separate trend line from the other penetrants. This result suggests perfluorocarbons experience a more favorable mixing process with fluorinated TFE/BDD87 than the other penetrants.

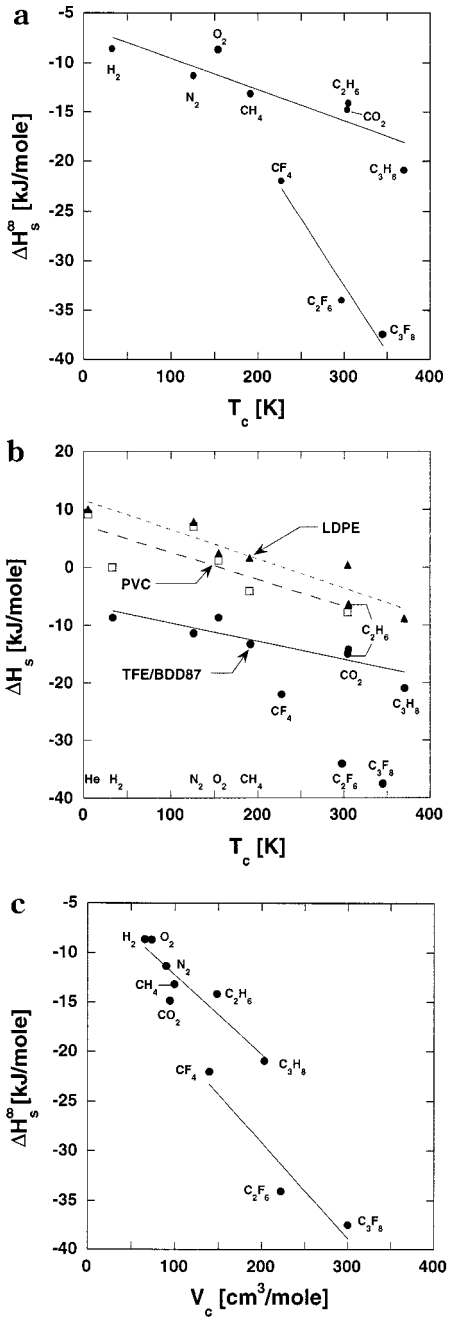

Figure 4. (a) Enthalpy of sorption in TFE/BDD as a function of penetrant critical temperature. (b) Comparison of enthalpies of sorption in TFE/BDD87 [●], rubbery low-density polyethylene [LDPE] [▲],[3] and glassy poly(vinyl chloride) [PVC] [□].[3] (c) Enthalpy of sorption in TFE/BDD as a function of penetrant size.

Figure 4b compares enthalpies of sorption in TFE/BDD87, rubbery, low-density polyethylene [LDPE], and glassy, poly(vinyl chloride) [PVC]. As described previ-

ously, the presence of nonequilibrium excess free volume (Langmuir microvoids) in glassy polymers allows penetrant molecules to be accommodated in a glassy matrix without requiring a large endothermic contribution to the creation of a molecular sized gap. Consequently, as demonstrated in Figure 4b, enthalpies of sorption are more exothermic in glassy TFE/BDD87 and PVC than in rubbery LDPE. Among the two glassy polymers, enthalpies of sorption are more exothermic in TFE/BDD87 than in PVC. This result likely reflects the greater amount of excess free volume possessed by and the lower cohesive energy density of TFE/BDD87 relative to PVC. The more excess free volume a polymer has, the more sorption sites are available that can accommodate penetrant molecules without requiring the creation of gaps in the polymer. TFE/BDD87 has a high excess free volume fraction (0.21 based on volume dilatometry estimates),[7] while the excess free volume fraction of PVC is only 0.03 based on carbon dioxide sorption data.[29] For penetrant molecules that partition into the densified matrix, the energy required to mix penetrant and polymer is proportional to the mismatch in their solubility parameters.[17] All of the penetrants examined in this study have solubility parameters lower than that of TFE/BDD87 ($\delta = 8.2$ (cal/cm^3)$^{1/2}$),[30] while the solubility parameter of PVC is 9.4 (cal/cm^3)$^{1/2}$.[31] Therefore, the mismatch in solubility parameters between PVC and the penetrants is larger in each case than that between TFE/BDD87 and the penetrants. Consequently, more energy is required to sorb penetrants into the densified regions of PVC than into similar regions of TFE/BDD87.

Figure 4c presents enthalpies of sorption in TFE/BDD87 as a function of penetrant critical volume, a convenient measure of penetrant size. On the basis of the data in this figure, ΔH_S^∞ decreases with increasing penetrant size. Similar to the correlation with penetrant critical temperature, ΔH_S^∞ values for the fluorocarbons fall on a separate trend line from the other penetrants. In this case, however, the slopes of the two trend lines are nearly equal and appear only to be offset from one another. This result suggests penetrant size may be a better correlating parameter for ΔH_S^∞ than T_C. Moreover, penetrant−polymer interactions not strictly related to penetrant size are more favorable for fluorocarbons than for the other penetrants.

Previous results indicate that as penetrant size increases, ΔH_{mix} becomes more exothermic in glassy polymers provided that the penetrant size is smaller than the average free volume element in the polymer matrix.[26] Under these conditions, the mixing process is similar to that of gases in associated liquids, such as water, and can be described in terms of solution theory as the formation of interstitial solutions.[23] In contrast, mixing of penetrants in nonassociated liquids, such as hydrocarbons, or rubbery polymers typically exhibits no dependence of ΔH_{mix} on penetrant size and is described in solution theory as a displacement solution.[23] As the infinite dilution enthalpy of sorption data display a distinct dependence on penetrant size, these data are consistent with mixing of penetrants in a glassy polymer where the size of all the penetrants is small relative to the average size of free volume elements in the polymer.

The concentration dependence of the enthalpy of sorption may be calculated from solubility data at multiple temperatures according to the following relation:[32]

$$\left[\frac{\mathrm{d}\ln p}{\mathrm{d}(1/T)}\right]_C = \frac{\Delta H_S}{zR} \tag{14}$$

where ΔH_S, the enthalpy of sorption, is a measure of the difference in enthalpy between a penetrant molecule in the sorbed state and in the gaseous state at a fixed concentration. R is the universal gas constant, z is the gas compressibility factor, and T is absolute temperature. For each of the penetrants examined in this study, ΔH_S was calculated from the slope of a semilogarithmic plot of p vs $1/T$ and the appropriate value of z at 35 °C, the midpoint of the temperature range considered.

According to the dual-mode model of sorption in glassy polymers, two energetically distinct sorption sites are available to accommodate penetrant molecules: Henry's law and Langmuir sites. In the context of this model, the concentration dependence of the enthalpy of sorption reflects changes in the distribution of penetrant molecules between these two environments. As penetrant concentration in a glassy polymer increases, Langmuir microvoids become progressively more saturated. As these sites are filled, a greater fraction of penetrant molecules partition into the densified Henry's law regions of the polymer. Penetrant dissolution into Henry's law sites is more energetically demanding than sorption in microvoids since it requires the creation of a gap in the polymer matrix of sufficient size to accommodate a penetrant molecule. Therefore, the dual-mode model predicts that ΔH_S will increase (i.e., become less exothermic) with penetrant concentration until the Langmuir sites are saturated, at which time ΔH_S should reach an asymptotic value determined by the enthalpy of sorption in the densified matrix. Since ΔH_{cond} is independent of concentration, ΔH_{mix} will exhibit the same functional dependence on concentration as ΔH_S.

There are relatively few reports of enthalpies of sorption in glassy polymers as a function of penetrant concentration. In this regard, Koros et al.[32] have reported a minimum in the enthalpy of sorption at low penetrant concentrations for CO_2 sorption in poly(ethylene terephthalate) [PET]. Barrie et al. report similar shaped curves for C_3H_8 sorption in polycarbonate and polystyrene.[33] To account for this minimum, Koros et al. developed a model for the concentration dependence of ΔH_S based on the temperature dependence of the dual-mode sorption parameters. This model assumes that an apparent enthalpy, derived from a van't Hoff form of the temperature dependence of the Langmuir capacity parameter, contributes to the enthalpy of sorption. As the authors noted, this assumption is valid if the temperature dependence of C'_H is a result of variations in polymer−penetrant interactions with temperature. On the other hand, if the temperature dependence of C'_H is due to a reduction in the number of microvoids as the polymer's glass transition temperature is approached, as is commonly believed,[34] then a minimum in ΔH_S as a function of concentration cannot be explained by this model. Recently, Banerjee et al.[35] reported enthalpies of sorption for CO_2 in poly(dimethylsiloxane) and polycarbonate which are independent of concentration. This result for polycarbonate is only consistent with a multisite sorption model if the enthalpies of sorption are the same in all sites.

Figure 5a presents ΔH_S as a function of penetrant concentration in TFE/BDD87 for the light gases N_2, O_2, and CO_2. The uncertainty in these measurements, as determined by a propagation of errors analysis,[36] is

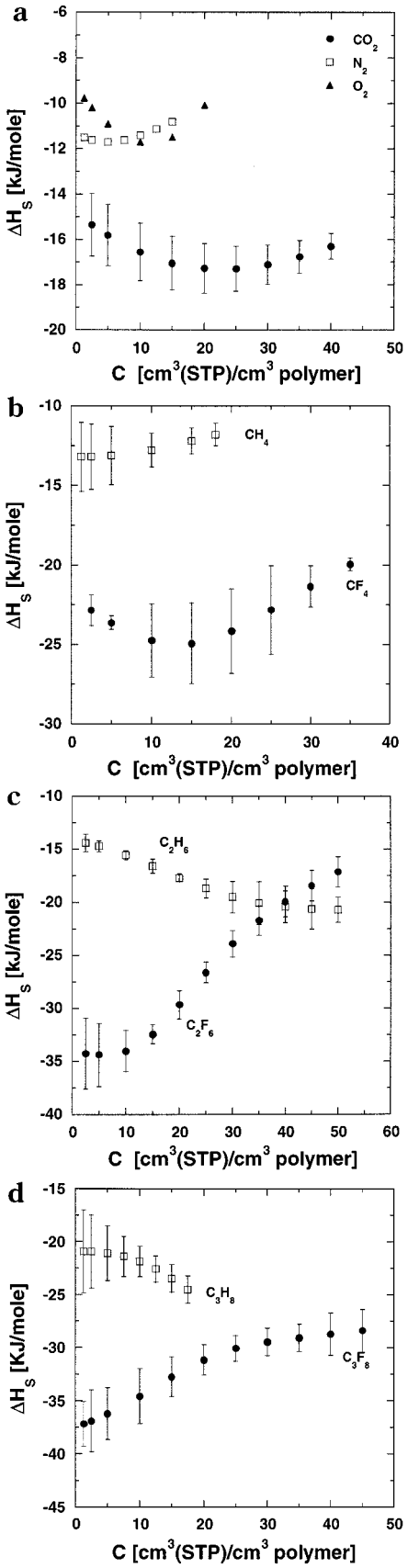

Figure 5. Enthalpies of sorption as a function of concentration in TFE/BDD87: (a) N_2, O_2, and CO_2; (b) CH_4 and CF_4; (c) C_2H_6 and C_2F_6; (d) C_3H_8 and C_3F_8.

±15% or less and is illustrated via error bars for CO_2. For the sake of clarity, error bars have been omitted from the N_2 and O_2 enthalpy of sorption data. For each of the light gas penetrants, ΔH_S is independent of concentration within experimental uncertainty. This result is consistent with that of Banerjee et al.[35] and suggests sorption of these light gases in TFE/BDD87 occurs in energetically equivalent sites over the range of concentrations examined.

Figure 5b presents ΔH_S as a function of penetrant concentration in TFE/BDD87 for CH_4 and CF_4. Similar to the light gases, ΔH_S is essentially independent of concentration for methane. For perfluoromethane, ΔH_S increases slightly as the concentration of this penetrant sorbed in TFE/BDD87 increases (for $C > 15$ cm^3 (STP)/cm^3). This result indicates that mixing CF_4 with TFE/BDD87 becomes energetically more difficult as penetrant concentration increases. This trend is consistent with the dual-mode interpretation of penetrant sorption and suggests once the most readily accessible sorption sites in TFE/BDD87 are filled by this large fluorocarbon penetrant, it becomes progressively more difficult to insert additional CF_4 molecules into the polymer matrix. Nevertheless, throughout the concentration range explored ΔH_S for CF_4 is substantially more exothermic than that of methane.

Figure 5c presents the concentration dependence of ΔH_S for C_2F_6 and C_2H_6. For perfluoroethane, the enthalpy of sorption increases as penetrant concentration in TFE/BDD87 increases. This result is similar to that observed for CF_4, although the concentration dependence is much stronger for C_2F_6. In contrast to its fluorocarbon analogue, the enthalpy of sorption for ethane decreases as concentration increases. Initially at infinite dilution, C_2H_6 molecules sorb into a fully fluorinated environment, which is likely to be an unfavorable process based on hydrocarbon−fluorocarbon liquid mixture interactions.[17] As the concentration of C_2H_6 increases, the average environment into which ethane molecules are dissolving is becoming chemically more like the penetrant itself, and therefore the mixing process becomes more favorable. This effect is apparently more important than that associated with the increase in enthalpy of sorption with concentration due to preferential filling of the energetically more accessible Langmuir sites at lower concentrations.

Figure 5d presents enthalpies of sorption as a function of concentration for C_3H_8 and C_3F_8. The behavior of these two penetrants is very similar to that of C_2F_6 and C_2H_6. Interestingly, for both pairs of analogues, the magnitude of the enthalpy of sorption at infinite dilution is approximately twice as great for the fluorocarbon penetrant as for the hydrocarbon penetrant, while at the highest concentrations examined, ΔH_S is, within experimental uncertainty, nearly equal for the fluorocarbon and hydrocarbon analogues. This result demonstrates that favorable interactions between TFE/BDD87 and the fluorocarbon penetrants are manifested primarily at low penetrant concentrations.

Permeability. Figure 6 presents the permeability of TFE/BDD87 to H_2, O_2, N_2, CO_2, CH_4, C_2H_6, C_3H_8, CF_4, C_2F_6, and C_3F_8 at 35 °C as a function of the pressure difference, Δp, across the polymer film. Consistent with previous studies, the permeability of TFE/BDD87 is very high compared to that of conventional polymers. For example, the permeability coefficient of oxygen in TFE/BDD87 (960 barrers) is nearly 3 orders of magnitude higher than it is in polycarbonate (1.4 barrers)[3], a conventional low free volume, amorphous glassy polymer. Table 4 compares permeability coefficients of light

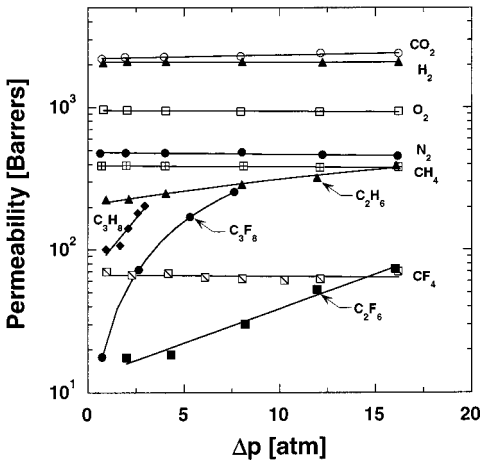

Figure 6. Permeability coefficients in TFE/BDD87 at 35 °C as a function of pressure difference.

Table 4. Comparison of Permeability Coefficients in TFE/BDD87

	permeability [barrers]			
penetrant	solution cast from PF 5060[a]	solution cast from PF 5052[b]	solution cast from perfluorotoluene[c]	melt pressed[d]
H_2	2100	3400	2400	2200
O_2	960	1600	1140	990
N_2	480	780	554	490
CO_2	2200	3900	2600	2800
CH_4	390	600	435	340
C_2H_6	210	370	252	180
CF_4	66			
C_2F_6	13			

[a] 35 °C and $\Delta p = 0$ (this work). [b] 25 °C, 50 psig upstream pressure, and 0 psig downstream pressure (Pinnau and Toy[10]). [c] 22−30 °C, 10−200 Torr upstream pressure, 10^{-4} Torr downstream pressure (Alentiev et al.[37]). [d] 25 °C, 65−270 psig upstream pressure, 0 psig downstream pressure (Nemser and Roman[6]).

gas and hydrocarbon penetrants measured in this work with those reported by other researchers. There is some scatter among permeability coefficients in TFE/BDD87 previously reported in the literature. In this regard, Alentiev et al.[37] have suggested that these permeability differences may be related to differences in film formation conditions. As demonstrated in Table 4, the permeability coefficients measured in this work are very similar to those reported by Nemser and Roman[6] for melt-pressed films and Alentiev et al.[37] for films cast from perfluorotoluene solutions. The permeability coefficients reported by Pinnau and Toy[10] are systematically higher by a factor of 1.7−2.0 than our values. This permeability difference suggests that the films of Pinnau and Toy were characterized by a more open polymer structure compared to our films, which, as we shall demonstrate later in this work, has ramifications for the activation energy of permeation.

As illustrated in Figure 6, the permeability coefficients of the light gases (H_2, O_2, N_2, CO_2) do not vary appreciably over the range of pressures explored in this study. This behavior is typical of supercritical, light gases in both rubbery and glassy polymers[1] and is consistent with the pressure dependence of permeability reported by Pinnau and Toy for permanent gases in TFE/BDD87.[10] Similar to the light gases, the permeability coefficients of CH_4 and CF_4 are independent of Δp. On the other hand, the permeability coefficients of the larger, more condensable hydrocarbon and fluorocarbon analogues (C_2H_6, C_3H_8, C_2F_6, and C_3F_8) increase significantly with increasing Δp, suggesting penetrant-induced plasticization of TFE/BDD87. For example, the permeability coefficient of C_3F_8 increases by a factor of 15 as Δp is increased from 0.7 to 7.6 atm. These results are consistent with those of Pinnau and Toy, who reported that TFE/BDD87 was easily plasticized by propane and chlorodifluoromethane.[10] On the basis of the data in Figure 6, the relative ease with which a penetrant plasticizes TFE/BDD87 is related to both penetrant size and solubility. Thus, for the penetrants that exhibit an increase in permeability with Δp, the relative magnitude of this increase follows the same order as penetrant solubility, i.e.: $C_2H_6 < C_2F_6 < C_3H_8 < C_3F_8$. The effect of size on a penetrant's ability to plasticize TFE/BDD87 is demonstrated by CO_2 and C_2H_6. While carbon dioxide is slightly more soluble than ethane in TFE/BDD87, the smaller size of the former apparently precludes it from introducing enough free volume into the polymer matrix to cause substantial plasticization under the conditions of our measurements.

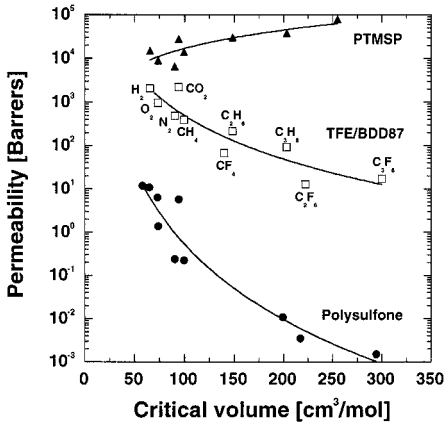

Figure 7. Permeability coefficients at 35 °C as a function of penetrant size in TFE/BDD87 [□], poly(1-trimethylsilyl-1-propyne) [PTMSP] [▲],[5] and polysulfone [●].[47]

Figure 7 presents permeability coefficients in TFE/BDD87 at $\Delta p = 0$ as a function of penetrant size. For comparison, permeability coefficients in polysulfone [PSF] and PTMSP for a similar range of penetrant sizes have been included in this figure. Frequently, there is a strong correlation between penetrant size and transport properties in both glassy and rubbery polymers.[38] In general, light gas (i.e., H_2, O_2, and N_2) permeability coefficients decrease with increasing penetrant size. Hydrocarbon vapor permeability increases with increasing penetrant size in rubbery or other weakly size-sieving polymers (i.e., PTMSP) and decreases with increasing penetrant size in strongly size-sieving, relatively low free volume glassy polymers such as PSF.[38] On the basis of the data in Figure 7, permeability coefficients in TFE/BDD87 are substantially higher than those in PSF but lower than those in PTMSP, the most permeable polymer known. The permeability of TFE/BDD87 generally decreases with increasing penetrant size, behavior consistent with that of a size sieving polymer such as PSF. However, over a similar range of penetrant sizes, permeability coefficients decrease by only 2 orders of magnitude in TFE/BDD87 as compared to 4 orders of magnitude in PSF. Additionally, the permeability coefficient of C_3F_8 is higher than that of C_2F_6 in TFE/BDD87, behavior characteristic of a weakly size-sieving polymer, such as PTMSP. Thus, TFE/

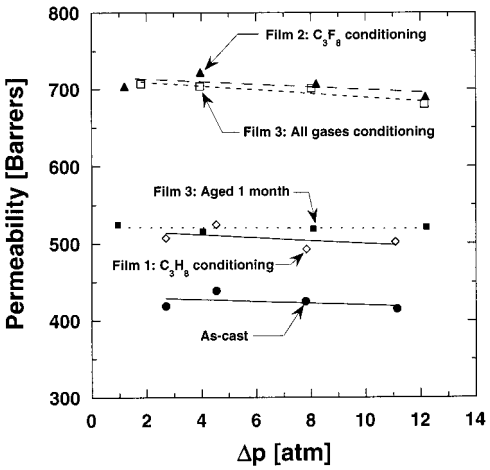

Figure 8. Nitrogen permeability coefficients in TFE/BDD87 at 25 °C as a function of film treatment history.

BDD87 exhibits permeability behavior intermediate between the extremes demonstrated by PSF and PTMSP.

Figure 8 presents the permeability of TFE/BDD87 films to nitrogen as a function of film treatment history. Three different films (labeled film 1, film 2, and film 3 in Figure 8) were utilized to obtain the data in this figure, and for each of these samples the as-cast nitrogen permeability was equal within experimental uncertainty. After film 1 was exposed to our highest available propane pressure (4.0 atm) overnight (approximately 16 h), the permeability of the film to nitrogen increased approximately 19%. Similarly, exposure of film 2 to perfluoropropane (pressure = 8.6 atm) overnight caused its permeability to nitrogen to increase by 66%. Film 3 was tested after it had been exposed to high pressures of all of the penetrants considered in this study. This film had nitrogen permeability coefficients essentially equal to those determined for film 2 after perfluoropropane exposure. Film 3 was then stored at ambient conditions for 1 month, at which time its permeability to nitrogen was measured again. After storage, its permeability to N_2 had decreased from 65% to only 23% higher than the as-cast value. These results indicate that TFE/BDD87 is susceptible to conditioning by exposure to highly soluble penetrant molecules. The level of conditioning, as measured by the effect on TFE/BDD87's permeability to nitrogen, is significantly greater after C_3F_8 exposure than after C_3H_8 exposure. This result is consistent with the higher solubility of perfluoropropane in TFE/BDD87 and the larger size of the fluorinated penetrant relative to its hydrocarbon analogue. Presumably the larger, more soluble C_3F_8 disrupts TFE/BDD87 chain packing more than C_3H_8. Thus, while both penetrants exhibit an ability to open the matrix, thereby increasing permeability, perfluoropropane does so to a greater extent. Interestingly, the N_2 permeability coefficients measured in this study after film exposure to C_3F_8 (or all of the penetrants) are similar to those reported by Pinnau and Toy for as-cast TFE/BDD87 films. This result indicates that through penetrant-induced structural rearrangement a single TFE/BDD87 sample can exist in several different quasi-equilibrium states, giving nitrogen permeabilities that span the range of literature values. Although the conditioned TFE/BDD87 structure is stable over the time scale of the permeability measurements, it does relax back toward an as-cast state over a much longer period of time (i.e., 1 month). This result is consistent with that reported by Jordan et al.[39] for CO_2 conditioning of polycarbonate and underscores the nonequilibrium nature of this glassy polymer.

Permeability coefficients for each of the penetrants examined, except the C_3 analogues, were determined as a function of temperature in TFE/BDD87. The activation energies of permeation, E_p, determined from the slope of Arrhenius plots of $\ln(P_0)$ vs $1/T$ are recorded in Table 3. For the penetrants considered in this study, the activation energies of permeation are positive since permeability increases with increasing temperature. This result is consistent with behavior observed in most glassy polymers but deviates from that reported by Pinnau and Toy[10] for TFE/BDD87. These researchers observed negative E_p values for N_2, O_2, and CO_2 in TFE/BDD87. This discrepancy is probably related to differences in the conditions of film formation between our samples and those of Pinnau and Toy. As discussed previously, the light gas and hydrocarbon permeability coefficients in TFE/BDD87 reported by Pinnau and Toy are systematically higher than ours, suggesting a more open polymer microstructure for their films. In a more open polymer matrix, less energy is required for a penetrant molecule to execute a diffusive jump. Therefore, the activation energies of diffusion and permeation (cf. eq 9) are lower than in a less open polymer matrix. In view of this consideration, higher E_p values in our TFE/BDD87 films as compared to Pinnau and Toy's should be expected on the basis of the relative permeability of these samples.

Figure 9a presents activation energies of permeation, E_p, as a function of penetrant Lennard-Jones diameter squared. Previous studies[40,41] indicate that the activation energy of diffusion increases linearly with the square of penetrant diameter in glassy polymers. In light of eq 9, a similar relationship should exist for E_p provided that $E_D > |\Delta H_S|$ and/or ΔH_S also scales with penetrant diameter squared. On the basis of the data in Figure 9a, activation energies of permeation in TFE/BDD87 correlate well with penetrant diameter squared. The greatest deviation from the trend line is observed for CO_2, which has an E_p value that falls below the best-fit line through all the penetrants. This result for CO_2 is consistent with that observed in other polymers (cf. Figure 9b). Carbon dioxide's nonspherical shape and relatively strong intermolecular interactions cause E_D to be small and the magnitude of ΔH_S to be large, respectively, compared to other similarly sized (as measured by V_C, kinetic diameter, etc.) penetrants. Figure 9b compares the effect of penetrant size on E_p in TFE/BDD87, polycarbonate, and PTMSP. The data for polycarbonate are typical for the effect of penetrant size on E_p for conventional glassy polymers: activation energies of permeation are positive because $E_D > |\Delta H_S|$, and they increase with increasing penetrant size, consistent with the functional dependence of E_D on penetrant size. In contrast, for PTMSP, activation energies of permeation are negative because $E_D < |\Delta H_S|$, and they become more exothermic as penetrant size increases, following the trend typically exhibited by ΔH_S with increasing penetrant size. This behavior is very unusual for dense, glassy polymer films and is similar to that observed in microporous solids, where the pore dimensions are large relative to the size of the penetrant molecules.[18] On the basis of the data in Figure 9b, TFE/BDD87 exhibits behavior intermediate between that of

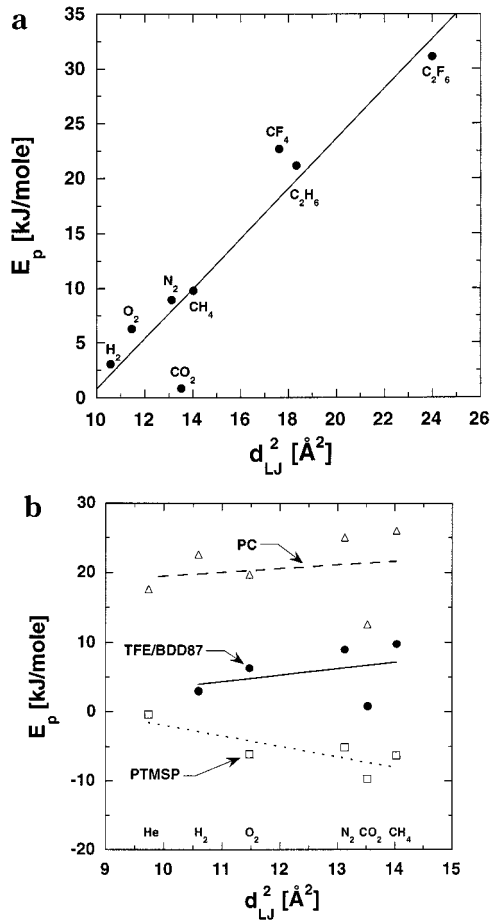

Figure 9. (a) Activation energy of permeation in TFE/BDD87 as a function of penetrant size. (b) Comparison of activation energies of permeation in low free volume polycarbonate [PC] [△][3] and high free volume poly(1-trimethylsilyl-1-propyne) [PTMSP] [□][16]and TFE/BDD87 [●].

polycarbonate and PTMSP. While E_p values in TFE/BDD87 are significantly lower than those in polycarbonate, they are nevertheless positive and increase with penetrant size. These results suggest that while TFE/BDD87 is endowed with a very open microstructure relative to conventional polymers, this structure probably does not constitute the series of interconnected gaps envisioned for PTMSP.[18]

Diffusivity. Concentration-averaged diffusion coefficients, $\bar{D}$, were estimated from the permeability and sorption data via the following rearranged form of eq 2:

$$\bar{D} = P\left(\frac{p_2 - p_1}{C_2 - C_1}\right) \tag{15}$$

where P is the pressure-dependent permeability coefficient measured at upstream and downstream pressures of p_2 and p_1, respectively, and C_1 and C_2 are the equilibrium penetrant concentrations sorbed in TFE/BDD87 at p_1 and p_2, respectively. The values of $\bar{D}$ represent local effective diffusion coefficients averaged over the concentration interval from C_1 to C_2, as indicated in eq 3.

Figure 10 presents calculated values of $\bar{D}$ as a function of penetrant concentration in TFE/BDD87 at 35 °C. The dual-mode transport model gives the

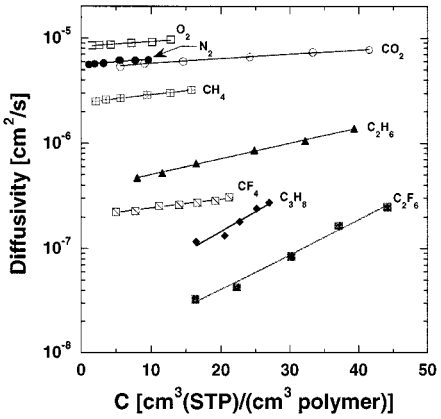

Figure 10. Concentration dependence of diffusion coefficients in TFE/BDD87 at 35 °C.

following relationship for the concentration dependence of $\bar{D}$:[1]

$$\bar{D} = \bar{D}_D\left[\frac{k_D + \dfrac{bC'_H\bar{D}_H/\bar{D}_D}{(1+bp_1)(1+bp_2)}}{k_D + \dfrac{C'_H b}{(1+bp_1)(1+bp_2)}}\right] \tag{16}$$

where $\bar{D}_D$ and $\bar{D}_H$ are the dual-mode diffusion coefficients in the Henry's law and Langmuir regions, respectively. According to this model, $\bar{D}$ should increase as penetrant concentration (or pressure) increases, since at higher pressures a greater fraction of penetrant molecules partition into the higher mobility Henry's law sites. The concentration dependence of $\bar{D}$ exhibited by O_2, N_2, CO_2, CH_4, and CF_4 is well-described by eq 16 with constant values of $\bar{D}_D$ and $\bar{D}_H$. This behavior is consistent with dual-mode transport in unplasticized glassy polymers.[1] For the larger, more soluble penetrants examined (C_2H_6, C_2F_6, and C_3F_8), $\bar{D}$ increases substantially as penetrant concentration increases. For example, the diffusion coefficient of C_2F_6 increases by nearly an order of magnitude over the range of penetrant concentrations investigated. This behavior cannot be described by eq 16 with constant values of $\bar{D}_D$ and $\bar{D}_H$ and suggests plasticization of TFE/BDD87 by these penetrants. This result in conjunction with the solubility data indicates that the dramatic increase in permeability coefficients observed for these penetrants with increasing Δp is primarily a result of increased penetrant mobility.

Figure 11 presents the effect of penetrant size on infinite dilution diffusion coefficients in TFE/BDD87. For comparison, diffusivity data in PTMSP and poly(vinyl chloride) [PVC] are also included in this figure. In general, diffusion coefficients in TFE/BDD87 decrease with increasing penetrant size, consistent with behavior typically observed in both glassy and rubbery polymers.[1] Diffusion coefficients in TFE/BDD87 are substantially higher than those in conventional, low free volume PVC. For the two high free volume polymers, PTMSP (FFV = 0.29[8]) and TFE/BDD87 (FFV = 0.32), diffusion coefficients are lower in TFE/BDD87 despite the similarity in FFV of these polymers. Previously,[42] higher transport parameters in PTMSP relative to TFE/BDD87 have been ascribed to free volume elements that may be more finely dispersed and isolated in TFE/BDD87 than in PTMSP. The diffusivity data for each of the

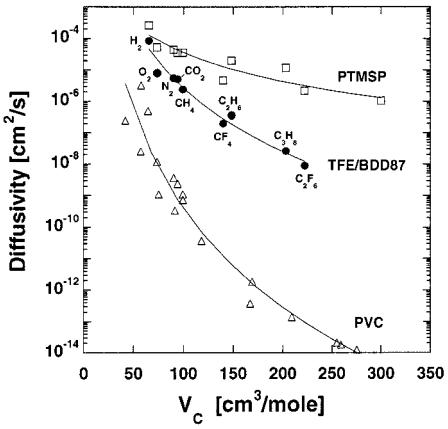

Figure 11. Diffusion coefficients in TFE/BDD87 [●], poly(vinyl chloride) [PVC] [△],[48] and poly(1-trimethylsilyl-1-propyne) [PTMSP] [□][5] as a function of penetrant size. The parameters in eq 16 for these polymers are $\tau = 36.8$, $\eta = 3.0$ [PTMSP]; $\tau = 6.8 \times 10^7$, $\eta = 6.7$ [TFE/BDD87]; and $\tau = 3.14 \times 10^{11}$, $\eta = 10.5$ [PVC].

three polymers in Figure 11 are well represented by the following relation, which is often used to correlate gas diffusion coefficients in liquids:[43]

$$D = \frac{\tau}{V_C^{\eta}} \tag{17}$$

where τ and η are adjustable parameters and V_C is penetrant critical volume. The lines through the experimental data in Figure 11 represent least-squares fits of this model to the data. The exponent in eq 17, η, is a measure of the size sieving ability of a polymer. Polymers with larger values of η exhibit diffusion coefficients that depend more strongly on penetrant size than polymers with smaller values of η. On the basis of the data in Figure 11, the values of η are 3.0 for PTMSP, 6.7 for TFE/BDD87, and 10.5 for PVC. In comparison, for a variety of low molar mass organic liquids, such as hexane and benzene, η is 0.45.[44] This result demonstrates that although TFE/BDD87 is a weakly size selective polymer relative to PVC, it nevertheless exhibits a greater propensity to separate molecules based on size than organic liquids or PTMSP.

From the E_p and ΔH_S values presented earlier, E_D values were calculated via eq 9. Figure 12a presents infinite dilution activation energies of diffusion, E_D, as a function of penetrant Lennard-Jones diameter squared. The error bars in this figure represent the uncertainty in the values of E_D as determined by a propagation of errors analysis.[36] As mentioned previously, activation energies of diffusion typically increase linearly with penetrant diameter squared in glassy polymers.[45] On the basis of the data in Figure 12a, this trend is obeyed. Carbon dioxide's E_D value does not deviate as far from the correlation line in Figure 12a as its E_p value does in Figure 9a, demonstrating the effect of this penetrant's relatively large $|\Delta H_S|$ value on E_p. For the rest of the penetrants, the deviation from the correlation lines in Figures 9a and 12a is similar, demonstrating that variations in E_p among penetrants are governed by changes in E_D (i.e., $E_D > |\Delta H_S|$). As illustrated in Figure 12b, activation energies of diffusion are lower in TFE/BDD87 and exhibit a weaker dependence on penetrant size as compared to those in polycarbonate. This result is consistent with the higher free volume and lower cohesive energy density in TFE/BDD87 than in PC. As

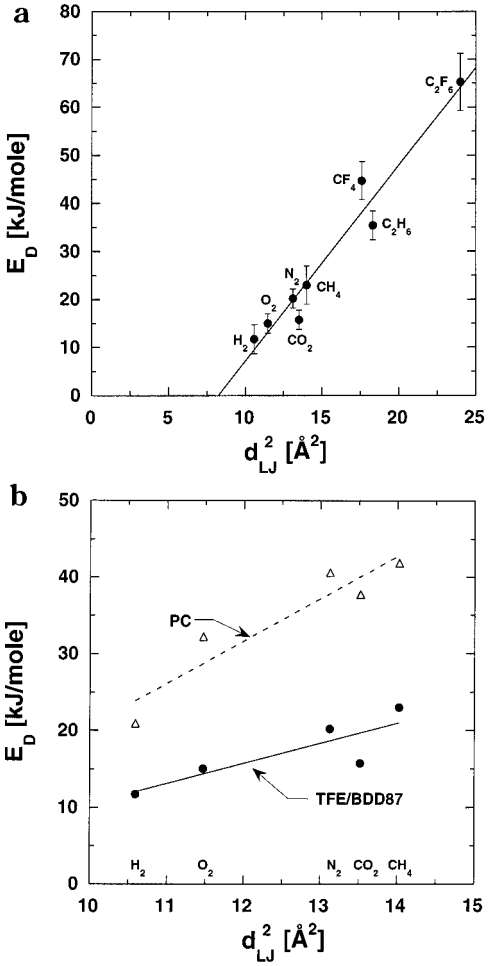

Figure 12. (a) Activation energy of diffusion at infinite dilution in TFE/BDD87 as a function of penetrant size. The equation for the best fit line through these data is $E_D = -33.6 + 4.1 d_{LJ}^2$. (b) Comparison of activation energies of diffusion in low free volume polycarbonate [PC] [△][3]and high free volume TFE/BDD87 [●].

cohesive energy increases, the slope of E_D vs d_{LJ}^2 should increase.[45] As free volume increases, E_D values are systematically reduced.[45]

Figure 13 presents D_0, the preexponential constant in eq 9, as a function of E_D/RT, a dimensionless form of the activation energy of diffusion. Previously, Van Amerongen[27] and Barrer and Skirrow[46] observed the following simple relationship between these variables:

$$\ln D_o = A\left(\frac{E_D}{RT}\right) - B \tag{18}$$

where both A and B are independent of penetrant type. Furthermore, A has a universal value of 0.64[46] independent of polymer type, and B has a value of $-\ln(10^{-4}$ cm^2/s$) = 9.2$ for rubbery polymers and $-\ln(10^{-5}$ cm^2/s$) = 11.5$ for glassy polymers.[28] This correlation is frequently described as a "linear free energy" relation.[45] The best-fit line through the TFE/BDD87 data in Figure 13 gives values of A and B equal to 0.63 ± 0.04 and 9.1 ± 0.5, respectively. Thus, the value of A for our TFE/BDD87 data is consistent with that in all other polymers. On the other hand, B for TFE/BDD87 is much lower than that reported for other glassy polymers and is comparable to the value of B for rubbery polymers. This result is consistent with the very high diffusivity

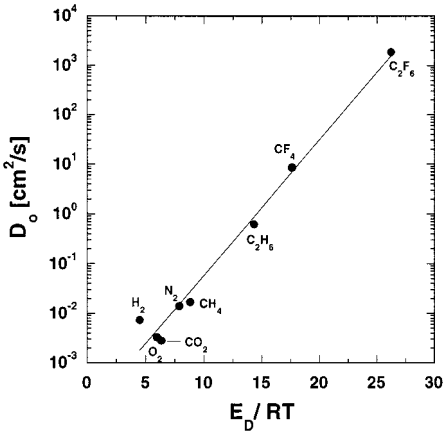

Figure 13. Linear free energy relation for TFE/BDD87. T = 308 K, the midpoint of the temperature range explored in this study.

values in TFE/BDD87, which are more comparable to diffusivities in rubbers than to those in conventional glassy polymers. The greatest deviation from the trendline in Figure 13 is observed for hydrogen, which has a higher D_0 value than expected on the basis of its activation energy. This result is consistent with that of Van Amerongen,[27] who observed high D_0 values for hydrogen in rubbery polymers.

Conclusions

Sorption isotherms of all penetrants except hydrogen in TFE/BDD87 are concave to the pressure axis and are well-described by the dual-mode model. Hydrogen exhibits linear sorption isotherms. In contrast to previous results in hydrocarbon-rich polymers, the solubility of perfluorocarbon penetrants is higher in TFE/BDD87 than that of their hydrocarbon analogues. On the basis of a corresponding states correlation of penetrant solubility with critical temperature, fluorocarbon penetrants experience more favorable interactions than their hydrocarbon analogues with perfluorinated TFE/BDD87. The solubility of all penetrants in TFE/BDD87 decreases with increasing temperature, indicating sorption occurs exothermically. Enthalpies of sorption in TFE/BDD87 correlate well with penetrant size, consistent with small molecule mixing in interstitial solutions. Fluorocarbon enthalpies of sorption at infinite dilution are significantly more exothermic than those of their hydrocarbon analogues in TFE/BDD87. ΔH_S is essentially independent of penetrant concentration for the smaller, less soluble penetrants examined in this study (O_2, N_2, CO_2, CH_4). For each of the fluorocarbon penetrants, ΔH_S becomes less exothermic as penetrant concentration increases, indicating the process of mixing these large penetrants with TFE/BDD87 becomes less favorable at high concentrations. Enthalpies of sorption of C_2H_6 and C_3H_8 decrease with increasing penetrant concentration, suggesting these penetrants are dissolving into a progressively more favorable environment. As a result of this different behavior, the enthalpies of sorption of the larger hydrocarbon and fluorocarbon analogues (C_2F_6/C_2H_6 and C_3F_8/C_3H_8) are nearly equal at high concentrations.

At low pressure, perfluorocarbon permeability coefficients are nearly an order of magnitude lower than those of their hydrocarbon analogues. In light of the higher fluorocarbon solubilities, this result is ascribed to the larger size of the fluorocarbons and their subsequently lower diffusivities in TFE/BDD87. TFE/BDD87 is easily plasticized by the larger, more soluble penetrants examined and is susceptible to penetrant-induced conditioning. The level of conditioning is highest for the largest, most soluble penetrant examined (C_3F_8), and although relatively long-lived, the conditioned state gradually relaxes back toward the as-cast state. The permeability of TFE/BDD87 increases with increasing temperature for all of the penetrants studied, indicating activation energies of permeation are positive. E_p values in TFE/BDD87 are relatively small compared to those in conventional glassy polymers, suggesting comparatively easy diffusion of penetrants in this high free volume polymer.

Diffusion coefficients of the lower sorbing gases examined (O_2, N_2, CO_2, CH_4, CF_4) exhibit concentration-dependent behavior consistent with dual-mode transport in unplasticized glassy polymers. For more strongly sorbing C_2H_6, C_3H_8, C_2F_6, and C_3F_8, diffusion coefficients increase rapidly with increasing penetrant concentration, indicating plasticization. Activation energies of diffusion in TFE/BDD87 are positive and increase linearly with penetrant diameter squared. In comparison to conventional glassy polymers, E_D values in TFE/BDD87 are low, indicating penetrants make diffusive jumps relatively easily in this high free volume polymer. Nevertheless, $|E_D|$ is larger than $|\Delta H_S|$ in TFE/BDD87, and therefore differences in E_D among penetrants govern trends in E_p.

Acknowledgment. The research described in this publication was made possible in part by Award No. RC2-347 of the U.S. Civilian Research and Development Foundation for the Independent States of the Former Soviet Union (CRDF). The authors also gratefully acknowledge partial support of this work by a grant from the U.S. National Science Foundation (CTS-9803225).

References and Notes

(1) Ghosal, K.; Freeman, B. D. *Polym. Adv. Technol.* **1994**, *5*, 673−697.
(2) Alsmeyer, Y. W.; Childs, W. V.; Flynn, R. M.; Moore, G. G. I.; Smeltzer, J. C. *Electrochemical Fluorination and Its Applications*; Plenum Press: New York, 1994.
(3) Pauly, S. *Permeability and Diffusion Data*; John Wiley & Sons: New York, 1989.
(4) Merkel, T. C.; Bondar, V.; Nagai, K.; Freeman, B. D. *J. Polym. Sci., Part B: Polym. Phys.*, in press.
(5) Merkel, T. C.; Bondar, V.; Nagai, K.; Freeman, B. D. *J. Polym. Sci., Part B: Polym. Phys.*, in press.
(6) Nemser, S. M.; Roman, I. A. Perfluorodioxole Membranes, US Patent No. 5,051,114, 1991.
(7) Resnick, P. R.; Buck, W. H. Teflon AF Amorphous Fluoropolymers. In Scheirs, J., Ed.; *Modern Fluoropolymers: High Performance Polymers for Diverse Applications*; John Wiley & Sons: New York, 1997; pp 397−419.
(8) Ichiraku, Y.; Stern, S. A.; Nakagawa, T. *J. Membr. Sci.* **1987**, *34*, 5−18.
(9) Ghosal, K.; Chern, R. T.; Freeman, B. D.; Savariar, R. *J. Polym. Sci., Part B: Polym. Phys.* **1995**, *33*, 657−666.
(10) Pinnau, I.; Toy, L. G. *J. Membr. Sci.* **1996**, *109*, 125−133.
(11) Cummins, W. R.; Dupuis, G.; Kesari, S.; Miner, D.; Trilli, K.; Fleming, G. *Semicond. Int.* **1997**, *20*, 265−272.
(12) Koros, W. J.; Chan, A. H.; Paul, D. R. *J. Membr. Sci.* **1977**, *2*, 165−190.
(13) Stern, S. A.; Gareis, P. J.; Sinclair, T. F.; Mohr, P. H. *J. Appl. Polym. Sci.* **1963**, *7*, 2035−2051.
(14) Sanders, E. S.; Koros, W. J.; Hopfenberg, H. B.; Stannett, V. T. *J. Membr. Sci.* **1984**, *18*, 53.
(15) Merkel, T. C.; Bondar, V.; Nagai, K.; Freeman, B. D. *Macromolecules* **1999**, *32*, 370−374.

(16) Masuda, T.; Iguchi, Y.; Tang, B.; Higashimura, T. *Polymer* **1988**, *29*, 2041−2049.
(17) Hildebrand, J. H.; Prausnitz, J. M.; Scott, R. L. *Regular and Related Solutions*; Van Nostrand Reinhold Company: New York, 1970.
(18) Srinivasan, R.; Auvil, S. R.; Burban, P. M. *J. Membr. Sci.* **1994**, *86*, 67−86.
(19) Gee, G. *Q. Rev., Chem. Soc.* **1947**, *1*, 265−298.
(20) Michaels, A. S.; Bixler, H. J. *J. Polym. Sci.* **1961**, *L*, 393−412.
(21) Stern, S. A.; Mullhaupt, J. T.; Gareis, P. J. *AIChE J.* **1969**, *15*, 64−73.
(22) Suwandi, M. S.; Stern, S. A. *J. Polym. Sci.* **1973**, *11*, 663−681.
(23) Bondar, V. I.; Freeman, B. D.; Yampolskii, Y. P. *Macromolecules* **1999**, *32*, 6163−6171.
(24) Vieth, W. R.; Howell, J. M.; Hsieh, J. H. *J. Membr. Sci.* **1976**, *1*, 177−220.
(25) Yampolskii, Y. P.; Kaliuzhnyi, N. E.; Durgarjan, S. G. *Macromolecules* **1986**, *19*, 846−850.
(26) Yampolskii, Y. P.; Volkov, V. V. *J. Membr. Sci.* **1991**, *64*, 191−228.
(27) Van Amerongen, G. J. *Rubber Chem. Technol.* **1964**, *37*, 1065−1152.
(28) Van Krevelen, D. W. *Properties of Polymers: Their Correlation with Chemical Structure; Their Numerical Estimation and Prediction from Additive Group Contributions*; Elsevier: Amsterdam, 1990.
(29) Collins, E. A.; Daniels, C. A.; Witenhafer, D. E. *Physical Constants of Poly(vinyl chloride)*; John Wiley & Sons: New York, 1989.
(30) Lawson, D. D. *Appl. Energy* **1980**, *6*, 241−255.
(31) Grulke, E. A. *Solubility Parameter Values*; John Wiley & Sons: New York, 1989.
(32) Koros, W. J.; Paul, D. R.; Huvard, G. S. *Polymer* **1979**, *20*, 956−960.
(33) Barrie, J. A.; Williams, M. J. L.; Munday, K. *Polym. Eng. Sci.* **1980**, *20*, 20−29.
(34) Koros, W. J.; Paul, D. R. *J. Polym. Sci., Part B: Polym. Phys. Ed.* **1981**, *19*, 1655−1656.
(35) Banerjee, T.; Chhajer, M.; Lipscomb, G. G. *Macromolecules* **1995**, *28*, 8563−8570.
(36) Bevington, P. R. *Data Reduction and Error Analysis for the Physical Sciences*; McGraw-Hill Book Company: New York, 1969.
(37) Alentiev, A. Y.; Yampolskii, Y. P.; Shantarovich, V. P.; Nemser, S. M.; Platé, N. A. *J. Membr. Sci.* **1997**, *126*, 123−132.
(38) Freeman, B. D.; Pinnau, I. *Trends Polym. Sci.* **1997**, *5*, 167.
(39) Jordan, S. M.; Koros, W. J.; Fleming, G. K. *J. Membr. Sci.* **1987**, *30*, 191−212.
(40) Meares, P. *J. Am. Chem. Soc.* **1954**, *76*, 3415−3422.
(41) Brandt, W. W. *J. Phys. Chem.* **1959**, *63*, 1080−1084.
(42) Freeman, B. D.; Hill, A. J. Free Volume and Transport Properties of Barrier and Membrane Polymers. In Tant, M. R., Hill, A. J., Eds.; *Structure and Properties of Glassy Polymers*; ACS Symposium Series No. 710; American Chemical Society: Washington, DC, 1999; pp 306−325.
(43) Freeman, B. D.; Pinnau, I. Membrane Materials Design Considerations for Gas Separations. In Freeman, B. D., Pinnau, I., Eds.; *Polymeric Membranes for Gas and Vapor Separations: Chemistry and Materials Science*; ACS Symposium Series No. 733; American Chemical Society: Washington, DC, 1999; pp 1−27.
(44) Reid, R. C.; Prausnitz, J. M.; Poling, B. E. *The Properties of Gases and Liquids*; McGraw-Hill: New York, 1987.
(45) Freeman, B. D. *Macromolecules* **1999**, *32*, 375−380.
(46) Barrer, R. M.; Skirrow, G. *J. Polym. Sci.* **1948**, *3*, 549−563.
(47) *Permeability and Other Film Properties Of Plastics and Elastomers*; Plastics Design Library: Norwich, NY, 1995.
(48) Berens, A. R.; Hopfenberg, H. B. *J. Membr. Sci.* **1982**, *10*, 283.

MA990685R